J. Fluid Mech. (1993), *vol.* 249, *pp.* 535–555

Axial dispersion in a channel with oscillating walls

By P. E. HYDON AND T. J. PEDLEY
Department of Applied Mathematical Studies, University of Leeds, Leeds LS2 9JT, UK

(Received 27 January 1992 and in revised form 17 November 1992)

An analysis is made of solute transport through a fluid within a long, but finite, channel or pipe whose walls remain parallel but oscillate transversely. When the fluid is viscous, the wall motion causes steady streaming. Axial dispersion of solute is calculated over a wide parameter range, and mean longitudinal transport is found to be greatly enhanced when the steady-streaming Reynolds number is much greater than unity. The results are applied to low-volume high-frequency ventilation of the human lung.

1. Introduction

The motivation for the present work is to improve understanding of gas transport in the airways of the lung. These are short, dichotomously (but asymmetrically) branching tubes, through which air is carried between the mouth and the terminal gas exchanging units, the alveoli. There are on average about twenty airway generations in the adult human lung, fewer on some pathways and more on others. The mean diameter and length of the airways decrease with distance from the trachea (the largest airway), although their total cross-sectional area increases rapidly with distance. The larger airways are lined with cartilage, so are less compliant than the smaller ones, whose diameter varies substantially during a breath.

It has been found (e.g. Bohn *et al.* 1980; Slutsky *et al.* 1980) that effective gas exchange in dogs can be maintained with tidal volumes that are significantly less than the volume of the conducting airway system, but only if the frequency of ventilation is substantially increased. Frequencies of up to 30 Hz are used in man, as compared with the normal resting breathing frequency of 0.25 Hz. This technique of artificial ventilation is called high-frequency ventilation (HFV).

Gas transport at low volumes and high frequencies may be enhanced by ventilation of alveoli supplied by short pathways and by 'pendelluft' (the sloshing of gas between neighbouring airways due to a mismatch in impedance), as discussed in the review by Slutsky, Kamm & Drazen (1985), but neither is sufficient to account for the fact that HFV can maintain adequate levels of oxygen and carbon dioxide in man at very low tidal volumes. It is clear that the interaction of diffusion and the highly unsteady flow in the conducting airways must be taken into account (Drazen, Kamm & Slutsky 1984).

The transport of a marker or passive solute in an incompressible fluid is governed by the advection–diffusion equation

$$\hat{C}_{\hat{t}} + \hat{\boldsymbol{u}} \cdot \hat{\boldsymbol{\nabla}} \hat{C} = \kappa \hat{\nabla}^2 \hat{C}, \tag{1.1}$$

where $\hat{C}$ is the concentration, $\hat{\boldsymbol{u}}$ is the fluid velocity and κ is the molecular diffusivity of the solute in the fluid. (A caret over a variable or operator signifies that it is dimensional; the same variable will be used for non-dimensional quantities, but with

the caret removed.) Suitable boundary conditions must be applied. If B is a fixed solid impermeable boundary with unit normal $\boldsymbol{n}$, then

$$\boldsymbol{n}\cdot\hat{\boldsymbol{\nabla}}\hat{C} = 0 \quad \text{on} \quad B. \tag{1.2}$$

In a finite tube, end conditions must also be considered. Typically, the concentration $\hat{C}$ or its axial gradient $\hat{C}_{\hat{x}}$ will be specified. The problem of choosing appropriate end conditions is discussed in §3.

The dispersion of a bolus of solute in a long rigid cylindrical tube was studied by Taylor (1953) and Aris (1956), who generalized Taylor's results. They concluded that if U_0 is the mean axial velocity, $\hat{z} = \hat{x} - U_0\,\hat{t}$, and a_0 is half of the typical tube width then the cross-sectionally averaged concentration, $\bar{\hat{C}}$, satisfies

$$\bar{\hat{C}}_{\hat{t}} = \kappa_{\text{eff}}\,\bar{\hat{C}}_{\hat{z}\hat{z}}, \tag{1.3}$$

where

$$\kappa_{\text{eff}} = \kappa(1+\gamma P^2), \tag{1.4}$$

$P = U_0\,a_0/\kappa$ is the Péclet number (the ratio of advective to diffusive terms in (1.1)), and γ is a positive number dependent upon the geometry of the tube ($\gamma = \frac{1}{48}$ for a rigid cylindrical tube; $\gamma = \frac{2}{105}$ for a parallel-sided, rigid two-dimensional channel). This result applies asymptotically, as $\hat{t} \to \infty$, and is independent of the initial distribution of solute.

Following Taylor's 1953 paper, many different dispersion problems have been analysed. Dispersion in a long rigid straight tube or channel when the flow is driven by an oscillatory axial pressure gradient is particularly relevant to the lung, and has been studied by Harris & Goren (1967), Chatwin (1975), and Watson (1983). Their results have been experimentally tested by Joshi *et al.* (1983), and were found to give reasonable agreement with experiment. The effects of tube curvature have been studied, both for steady flow (Erdogan & Chatwin 1967; Nunge, Lin & Gill 1972; Johnson & Kamm 1986) and for oscillatory flow (Eckmann & Grotberg 1988; Pedley & Kamm 1988; Sharp *et al.* 1991). In this case the velocity is not everywhere parallel to the tube axis, and the presence of secondary motions means that the fluid can, in certain circumstances, be transported across the tube cross-section more rapidly than by diffusion alone. In particular, a purely oscillatory axial flow generates transverse steady streaming (Lyne 1971).

In the above problems, the tube is uniform and the flow fully developed, so no axial steady streaming occurs, and the mean longitudinal solute flux consists of steady axial diffusion together a contribution from the interaction between the unsteady axial velocity and the unsteady concentration distribution. One non-uniformity found in airways is taper. The effect of oscillatory flow and gradual taper upon dispersion in a rigid axisymmetric tube has been studied by Godleski & Grotberg (1988). The non-uniformity of the tube requires the existence of transverse velocity components, which contribute to lateral mixing. There is also an axial component of steady-streaming velocity, which one might suppose would contribute to the axial solute flux. However, this is not the case (to leading order); the zero-order concentration field is uniform across the cross-section and the cross-sectional average of the steady streaming is zero, so there is no net axial advection of solute by the steady streaming.

The problem of transport during volume-cycled oscillatory flow in a thin-walled viscoelastic tube has been treated by Dragon & Grotberg (1991), who found that the solute flux is reduced as wall compliance increases, so that the dispersion produced is less than in a rigid tube. For soft tubes, the optimal dispersion is achieved when the phase difference between the wall motion and the forced motion of the fluid is minimized.

In the present paper, we consider how pulsation of the tube walls affects axial transport. Our analysis will be restricted to the case of the mixing of one gas in another, for which the Schmidt number $\sigma = \nu/\kappa$ is $O(1)$ (ν being the kinematic viscosity), but may readily be extended to large σ and applied to the mixing of solutes in liquids. We examine the effect of wall oscillations by studying a model problem in a finite tube, whose wall remains rigid and parallel whilst oscillating transversely. The principal conclusion of the present work, in contrast to those of Godleski & Grotberg and Dragon & Grotberg, will be that the axial steady streaming dominates the dispersion process when the Péclet number based upon the steady streaming velocity is sufficiently large.

2. Formulation of the model problem

We now investigate the way in which transverse parallel oscillations of a tube wall generate a flow which enhances solute dispersion. The simplest geometry in which to analyse such dispersion is a two-dimensional channel. Accordingly, the main discussion in each section treats the two-dimensional problem. The corresponding results for an axisymmetric tube are calculated similarly, and are presented without derivation (details may be obtained from the authors).

We study dispersion in a long straight channel with a large tank of fluid at each end (figure 1). The channel walls are at $\hat{y} = \pm\hat{a}(\hat{t})$, where

$$\hat{a}(\hat{t}) = a_0(1+\epsilon\cos\omega\hat{t}). \tag{2.1}$$

It is assumed that $\epsilon \ll 1$. The ends of the channel are at $\hat{x} = a_0 l$ and $\hat{x} = a_0 L$, where $l < 0 < L$ and $L-l \gg 1$. Secomb (1978) has analysed the flow in an infinite channel whose walls oscillate according to (2.1). It is reasonable to assume that the flow in a long finite channel will be very closely approximated by Secomb flow away from the channel ends. Since it is not the purpose of this work to study entry or exit effects upon the dispersion, we will assume that the flow in the channel is everywhere equal to that calculated by Secomb.

The tanks at $\hat{x} = a_0 l$ and $\hat{x} = a_0 L$ contain fluid with solute concentrations $\hat{C}_l$ and $\hat{C}_L$ respectively. Without loss of generality, we suppose that $\hat{C}_L > \hat{C}_l$. The fluid within each tank is well mixed, and the tanks are assumed to be so large that the tank concentrations do not change noticeably over a cycle.

We look for solutions of the advection–diffusion equation which are periodic, so that any transients resulting from a particular choice of initial conditions will have been attenuated. In particular, when there is no fluid flow and the walls are fixed at $\hat{y} = a_0$, the concentration will be steady, varying linearly with $\hat{x}$:

$$\hat{C}(\hat{x},\hat{y},\hat{t}) = \frac{1}{a_0 L - a_0 l}[a_0 L\hat{C}_l - a_0 l\hat{C}_L + (\hat{C}_L - \hat{C}_l)\hat{x}]. \tag{2.2}$$

In this case, the solute flux across a cross-section (i.e. a plane $x =$ constant) is independent of time:

$$\mathscr{F}_0 = \frac{-2\kappa(\hat{C}_L - \hat{C}_l)}{L-l}. \tag{2.3}$$

$\mathscr{F}_0$ is the solute flux per unit channel breadth in the positive $\hat{x}$-direction.

When there is a fluid flow, the time-averaged flux across a cross-section is

$$\hat{\mathscr{F}} = \left\langle \int_{-\hat{a}(\hat{t})}^{\hat{a}(\hat{t})} (\hat{u}\hat{C} - \kappa\hat{C}_{\hat{x}})\,\mathrm{d}\hat{y} \right\rangle, \tag{2.4}$$

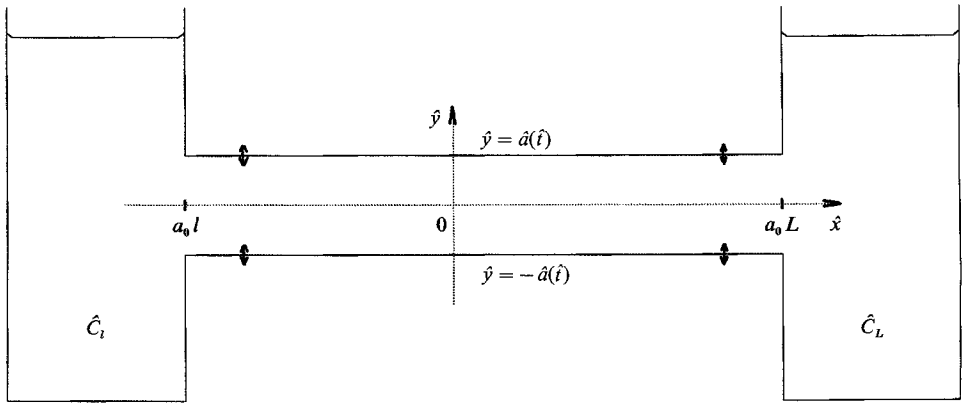

FIGURE 1. Geometry of the model problem (see text).

where $\hat{u}$ is the $\hat{x}$-component of velocity. It turns out that the dispersion produced by transverse parallel-wall oscillation is not a Gaussian process, even in a time-averaged sense, so it is not possible to model it by a one-dimensional diffusion equation with an effective diffusivity. However, the relative increase in transport across a cross-section,

$$\mathscr{R} = \hat{\mathscr{F}}/\mathscr{F}_0 - 1, \tag{2.5}$$

is a measure of the effect of the fluid flow on the transport of solute. The use of $\mathscr{R}$ to characterize the dispersion is consistent with Watson (1983).

In Secomb's (1978) solution, the transverse velocity $\hat{v}$, equal to $\pm\hat{a}_{\hat{t}}$ at $\hat{y} = \pm\hat{a}(\hat{t})$, is independent of $\hat{x}$. Therefore (from continuity) the axial velocity $\hat{u}$ is linear in $\hat{x}$ and (from the $\hat{x}$-momentum equation) the pressure gradient is quadratic, that is

$$\hat{u}(\hat{x}, \hat{y}, \hat{t}) = \hat{u}_0(\hat{y}, \hat{t}) + \hat{x}\hat{u}_1(\hat{y}, \hat{t}), \tag{2.6}$$

$$\hat{p}(\hat{x}, \hat{y}, \hat{t}) = \hat{x}^2\hat{p}_2(\hat{t}) + \hat{x}\hat{p}_1(\hat{t}) + \hat{p}_0(\hat{y}, \hat{t}) \tag{2.7}$$

($\hat{p}_1$ and $\hat{p}_2$ are functions of $\hat{t}$ only, from the $\hat{y}$-momentum equation). Different powers of $\hat{x}$ in the Navier–Stokes equations lead to a set of equations for $\hat{u}_0$, $\hat{u}_1$, $\hat{v}$, $\hat{p}_0$, $\hat{p}_1$ and $\hat{p}_2$ in terms of $\hat{t}$ and $\hat{y}$. However, $\hat{u}_1$, $\hat{v}$, and $\hat{p}_2$ can be determined independently of the other variables, and will be referred to as the 'wall-driven flow'. The $\hat{x}$-independent axial velocity $\hat{u}_0$, although influenced by $\hat{u}_1$ and $\hat{v}$, can be regarded as driven by the $\hat{x}$-independent part of the pressure gradient, $\hat{p}_1$, and is zero if $\hat{p}_1$ is zero. In this paper we analyse dispersion in wall-driven flow, with $\hat{u}_0 \equiv 0$. The problem with a pressure-driven flow will be studied in a subsequent paper.

It is helpful to choose a frame of reference in which the walls are fixed. Accordingly, Secomb chose the (non-dimensional) transverse variable to be

$$\eta = \hat{y}/\hat{a}(\hat{t}). \tag{2.8}$$

The other dimensionless variables are taken to be

$$x = \frac{\hat{x}}{a_0}, \quad t = \omega\hat{t}, \quad u_1 = \frac{\hat{u}_1}{\omega}, \quad v = \frac{\hat{v}}{a_0\omega}, \quad \phi_2 = \frac{\hat{p}_2}{\rho\omega^2}, \quad a(t) = \frac{\hat{a}}{a_0}; \tag{2.9}$$

the only dimensionless constant appearing in the equations is the Womersley number $\alpha = a_0(\omega/\nu)^{\frac{1}{2}}$.

Assuming that the amplitude parameter, ϵ, was small, Secomb expanded all variables in powers of ϵ, with appropriate time-dependence at each order; for example,

$$v(\eta, t) = \epsilon\,\mathrm{Re}\{v^{11}(\eta)\,\mathrm{e}^{\mathrm{i}t}\} + \epsilon^2[v^{20}(\eta) + \mathrm{Re}\{v^{22}(\eta)\,\mathrm{e}^{2\mathrm{i}t}\}] + O(\epsilon^3). \tag{2.10}$$

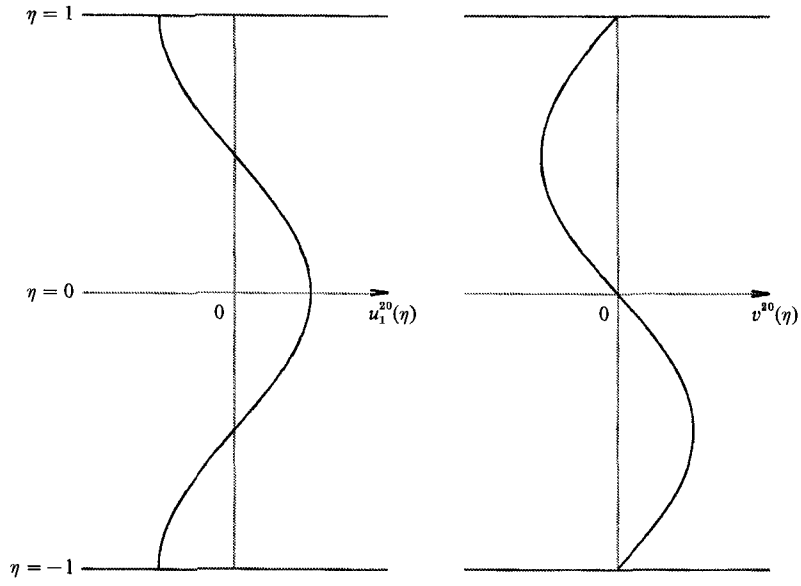

FIGURE 2. Steady streaming when $\alpha \gg 1$.

The variables u_1 and ϕ_2 have expansions of the same form, and the same superscript notation will be used throughout. The time-independent terms of $O(\epsilon^2)$ represent the steady streaming, which arises from the convective inertia term in an x-dependent flow.

When the steady-streaming Reynolds number $R_S = \epsilon^2\alpha^2$ is much less than unity, it is possible to carry out a uniform series expansion of the governing equations by comparing powers of ϵ. The resulting hierarchy of ordinary differential equations for $u_1^{ij}(\eta)$, $v^{ij}(\eta)$ and ϕ_2^{ij} is solved sequentially. We will require explicit expressions for the axial oscillatory flow u_1^{11} and the axial steady streaming u_1^{20} in order to determine the leading-order contribution to the solute dispersion. As calculated by Secomb, these are

$$u_1^{11} = (\mathrm{i}/D)(\cosh\beta\eta - \cosh\beta), \tag{2.11}$$

$$u_1^{20} = (1/8D\bar{D})\,\mathrm{Re}\{2\sinh\beta\eta\sinh\bar{\beta}\eta - 6\sinh\beta\sinh\bar{\beta} + 4\eta\sinh\beta\eta\sinh\bar{\beta} + 8\mathrm{i}\cosh\beta\eta\cosh\bar{\beta} + 3(\eta^2-1)\sinh\bar{\beta}[(11/\beta)\cosh\beta - 3\sinh\beta]\}, \tag{2.12}$$

where we use the notation $\beta = ((1+\mathrm{i})/\sqrt{2})\,\alpha$, $D = \cosh\beta - (1/\beta)\sinh\beta$; an overbar denotes the complex conjugate of a variable or parameter. The Fourier series representation of u_1^{11} will also be found useful:

$$u_1^{11} = -\mathrm{i} + \frac{2\mathrm{i}\beta\sinh\beta}{D}\sum_{n=1}^{\infty}\frac{(-1)^n}{n^2\pi^2+\beta^2}\cos n\pi\eta. \tag{2.13}$$

In addition, we shall need the leading-order term in the expansion for ϕ_2:

$$\phi_2^{11} = -(1/2D)\cosh\beta. \tag{2.14}$$

As α becomes large, variations in the axial oscillatory flow become confined to Stokes layers at the walls. The steady streaming is driven by the flow in the Stokes layers, and is directed towards $x = 0$ close to the walls and away from $x = 0$ in the centre of the channel (figure 2).

When $R_S > 1$ as $\epsilon \to 0$, the convective inertia of the steady streaming becomes comparable with the mean viscous force, so that the series solution above becomes

non-uniform. In this case, Secomb wrote $\alpha = N\epsilon^{-(1+c)}$, where $c \geqslant 0$ and $N = O(1)$ as $\epsilon \to 0$; the equations of motion are now singular, but may be solved using a boundary-layer analysis. The variables u_1, v and ϕ_2 are written as the sum of the solution for an inviscid fluid and the viscous perturbation:

$$u_1(\eta, t) = -\frac{a_t}{a} - a^2 F_\eta(\eta, t), \quad v(\eta, t) = a_t \eta + a^3 F(\eta, t), \quad \phi_2 = a_{tt}/2a - a_t^2/a^2 + \tilde{\phi}_2. \tag{2.15a–c}$$

The equation for the new dependent variable, $F(\eta, t)$, can be solved separately in the core and in the Stokes layers by expansion in powers of ϵ, and the solutions are matched in the usual way. It turns out that F^{11}, F^{22} and F^{31} are zero within the core, and the equation determining the steady streaming in the core has the analytic solution

$$F^{20} = -(3/4\pi) \sin \pi\eta \tag{2.16}$$

for $c > 0$. This solution was discussed in detail by Secomb (1978), who also solved the problem $c = 0$ numerically. The $c = 0$ solution matches the $R_S \ll 1$ solution as $N \to 0$, and matches the $c > 0$ solution as $N \to \infty$. We will use Secomb's results in our analysis of dispersion in the limiting cases $R_S \ll 1$ and $R_S \gg 1$ ($c > 0$). We will not treat the case $R_S = O(1)$ ($c = 0$) explicitly, but we note from Secomb (1978) that the velocity profile when $R_S = O(1)$ is similar in shape and magnitude to the profile when $R_S \gg 1$.

The (non-dimensional) instantaneous volume flux (per unit breadth) $Q(x, t)$ across a cross-section may be calculated from the continuity equation

$$u_1 + (1/a) v_\eta = 0, \tag{2.17}$$

together with the kinematic boundary conditions and is found to be

$$Q(x, t) = 2\epsilon x \sin t. \tag{2.18}$$

3. Equation and boundary conditions

We assume that the solute is passive and is transported by molecular diffusion and advection according to (1.1), which may be written

$$\theta_t + x u_1 \theta_x + \frac{v - a_t \eta}{a} \theta_\eta = \frac{1}{\alpha^2 \sigma} \left(\theta_{xx} + \frac{1}{a^2} \theta_{\eta\eta} \right), \tag{3.1}$$

using the non-dimensional variables introduced in §2, together with the non-dimensionalized concentration

$$\theta(x, \eta, t) = \frac{L - l}{\hat{C}_L - \hat{C}_l} \left[\hat{C} - \frac{L\hat{C}_l - l\hat{C}_L}{L - l} \right]. \tag{3.2}$$

This choice of non-dimensional concentration results in a unit concentration gradient when there is no flow; the equilibrium solute distribution is

$$\theta = x. \tag{3.3}$$

The fluid in the tanks at $x = l$ and L has concentration l and L respectively, so for a long channel, $|\theta|$ will be large, at least at one end.

The wall-driven velocity field can be written as a power series in ϵe^{it}, so we expect that the time-periodic solution of (3.1) will be of the form

$$\theta(x,\eta,t) = \theta^{00}(x,\eta) + \epsilon \operatorname{Re}\{\theta^{11}(x,\eta)\,e^{it}\} + \epsilon^2[\theta^{20}(x,\eta) + \operatorname{Re}\{\theta^{22}(x,\eta)\,e^{2it}\}] + O(\epsilon^3). \tag{3.4}$$

The solution is determined by the application of suitable boundary conditions. The walls at $\eta = \pm 1$ are solid and impermeable; hence

$$\theta_\eta = 0 \quad \text{at} \quad \eta = \pm 1. \tag{3.5}$$

The question of suitable conditions at the ends $x = l$ and L is more difficult; various end conditions have been adopted by workers in the field. Much of the work on shear dispersion has been applied to chemical flow reactors, in which it has usually been assumed that the flow is steady and x-independent, and that a one-dimensional advection–reaction–diffusion equation is a valid model (Danckwerts 1953; Wehner & Wilhelm 1956; Deckwer & Mählmann 1976). End conditions suitable for the lung during normal ventilation have been proposed by Butler (1977).

Smith (1988) found that, when advection dominates molecular diffusion, the one-dimensional model equation is inadequate close to any rapid transition in parameters, so that the entry and exit conditions must be determined from the full three-dimensional advection–reaction–diffusion equation. He derived such conditions for the one-dimensional model equation and the solution of that was in good agreement with the solution of the full three-dimensional problem sufficiently far downstream. However, for slowly varying or steady flows, and no reaction, the conditions proposed by Danckwerts proved to be appropriate. Since we ignore the details of the velocity field at the junctions between the channel and the tanks, we are also justified in using end conditions similar to those of Danckwerts, as set out below.

When both terms on the right-hand side of (3.1) are typically small compared with those on the left-hand side, advection is the chief mechanism of solute transport. The leading-order equation for the concentration is hyperbolic, and may be solved by the method of characteristics. We assume that, in these circumstances, no boundary layers exist at the ends. During inflow, the direction of propagation is from each tank into the channel, so we expect that the concentration at $x = L$ will equal that in the tank. During outflow, the direction of propagation is reversed, and so the concentration at $x = L$ is determined by the concentration within the channel at earlier times.

When the terms on the right-hand side of (3.1) are not negligible (to leading order), the equation is parabolic, and we assume that the mixing within each tank is sufficiently rapid that the problem may be treated as a boundary value problem, with the concentration at $x = L$ being equal to the tank concentration over the whole cycle.

The end conditions to be applied are therefore determined by the Péclet number based upon the steady part of the axial velocity, $P_S = \epsilon^2\alpha^2\sigma(L-l)^2$, which is an estimate of the ratio of the mean advected flux to the mean diffusive flux. We will assume that the same conditions may be applied to $x = l$ as to $x = L$. When $P_S \ll 1$ we impose

$$\theta = L \quad \text{at} \quad x = L, \qquad \theta = l \quad \text{at} \quad x = l, \quad \text{for all} \quad t. \tag{3.6a}$$

When $P_S \gg 1$, the end conditions are

$$\theta = L \quad \text{at} \quad x = L, \qquad \theta = l \quad \text{at} \quad x = l \quad \text{when} \quad (2n-1)\pi < t < 2n\pi \tag{3.6b}$$

for integer n, i.e. during inflow; no end conditions can be applied during the outflow half of the cycle. Equations (3.1), (3.5) and (3.6) constitute the boundary value problem

for transport of solute in the purely wall-driven flow. We shall investigate the parametric extremes, expecting that for intermediate values of the parameters an intermediate level of dispersion will occur. Therefore, we solve the problem for $P_S \ll 1$ in §4. The case $P_S \gg 1$ will be treated in §5.

4. Dispersion in a channel: small mean Péclet number

We now examine dispersion when $P_S \ll 1$, and so $R_S = \epsilon^2\alpha^2 \ll 1$. We seek a regular series solution of the form (3.4) to the advection–diffusion equation (3.1) subject to the no-flux condition at the walls (3.5) and the fixed end-concentration condition (3.6*a*). The leading-order part of the concentration is equal to that when there is no wall motion ($\epsilon = 0$), that is

$$\theta^{00} = x. \tag{4.1}$$

The equation for θ^{11} is

$$(1/\alpha^2\sigma)(\theta^{11}_{xx} + \theta^{11}_{\eta\eta}) - \mathrm{i}\theta^{11} = xu_1^{11} \tag{4.2}$$

subject to $$\theta^{11}_\eta = 0 \quad \text{at} \quad \eta = \pm 1, \qquad \theta^{11} = 0 \quad \text{at} \quad x = l, L, \tag{4.3}$$

which cannot be solved in closed form, but may be expressed as a Fourier series in η. Substituting (2.15) into (4.2) leads to the solution

$$\theta^{11} = G(x;\psi_0) - \frac{2\beta^3\sigma\sinh\beta}{D}\sum_{n=1}^{\infty}\frac{(-1)^n G(x;\psi_n)\cosh n\pi\eta}{\psi_n^2(n^2\pi^2+\beta^2)}, \tag{4.4}$$

where $$G(x;\psi_n) = x - L\frac{\sinh\psi_n(x-l)}{\sinh\psi_n(L-l)} - l\frac{\sinh\psi_n(L-x)}{\sinh\psi_n(L-l)} \tag{4.5}$$

and $\psi_n = (n^2\pi^2+\beta^2\sigma)^{\frac{1}{2}}$, $\mathrm{Re}\{\psi_n\} > 0$. We could go on to solve for θ^{20} in the same way, but that is not necessary for calculating the mean relative increase in solute flux across a cross-section, $\mathscr{R}$:

$$\mathscr{R} = \frac{\epsilon^2}{2}\int_{\eta=-1}^{1}(\theta_x^{20} + \tfrac{1}{2}\mathrm{Re}\{\theta_x^{11} - \alpha^2\sigma x\bar{u}_1^{11}\theta^{11}\})\,\mathrm{d}\eta + O(\epsilon^4). \tag{4.6}$$

This integral may be evaluated by averaging the equation for θ^{20},

$$\frac{1}{\alpha^2\sigma}(\theta^{20}_{xx} + \theta^{20}_{\eta\eta}) = \tfrac{1}{2}\mathrm{Re}\left\{x\bar{u}_1^{11}\theta_x^{11} + 2xu_1^{20} + (\bar{v}^{11} + \mathrm{i}\eta)\theta_\eta^{11} + \frac{2}{\alpha^2\sigma}\theta^{11}_{\eta\eta}\right\}, \tag{4.7}$$

across the cross-section:

$$\int_{\eta=-1}^{1}(\theta^{20}_{xx} + \tfrac{1}{2}\mathrm{Re}\{\theta^{11}_{xx}\})\,\mathrm{d}\eta = \frac{\alpha^2\sigma}{2}\int_{\eta=-1}^{1}\mathrm{Re}\{\bar{u}_1^{11}\theta^{11} + x\bar{u}_1^{11}\theta_x^{11}\}\,\mathrm{d}\eta. \tag{4.8}$$

The expansion of the continuity equation (2.17) leads to

$$u_1^{11} + v_\eta^{11} = 0, \tag{4.9}$$

$$u_1^{20} + v_\eta^{20} + \tfrac{1}{2}\mathrm{Re}\{u_1^{11}\} = 0, \tag{4.10}$$

which were used together with the boundary conditions on the flow to arrive at (4.8). Integrating (4.8) once with respect to x gives

$$\int_{\eta=-1}^{1}(\theta_x^{20} + \tfrac{1}{2}\mathrm{Re}\{\theta_x^{11}\})\,\mathrm{d}\eta = \frac{\alpha^2\sigma}{2}\int_{\eta=-1}^{1}\mathrm{Re}\{x\bar{u}_1^{11}\theta^{11}\}\,\mathrm{d}\eta + 2A, \tag{4.11}$$

where A is a constant of integration. Comparison with (4.6) shows that

$$\mathscr{R} = \epsilon^2 A + O(\epsilon^4). \tag{4.12}$$

The value of A may be found by integrating (4.11) again and applying the end conditions (4.3) and

$$\theta^{20} = 0 \quad \text{at} \quad x = l, L. \tag{4.13}$$

We obtain

$$A = \frac{-\alpha^2\sigma}{4(L-l)} \int_{x=l}^{L} \int_{\eta=-1}^{1} \mathrm{Re}\{x\bar{u}_1^{11}\theta^{11}\}\,\mathrm{d}\eta\,\mathrm{d}x, \tag{4.14}$$

which can be evaluated using (2.15) and (4.4). We can also show that $A > 0$ for all parameter values by using (4.2) to substitute for u_1^{11} in (4.14), yielding

$$A = \frac{-1}{4(L-l)} \int_{x=l}^{L} \int_{\eta=-1}^{1} \mathrm{Re}\{(\bar{\theta}_{xx}^{11} + \bar{\theta}_{\eta\eta}^{11})\theta^{11}\}\,\mathrm{d}\eta\,\mathrm{d}x, \tag{4.15}$$

which may be integrated by parts (using the end conditions (4.3)) to obtain

$$A = \frac{1}{4(L-l)} \int_{x=l}^{L} \int_{\eta=-1}^{1} (|\theta_x^{11}|^2 + |\theta_\eta^{11}|^2)\,\mathrm{d}\eta\,\mathrm{d}x, \tag{4.16}$$

which is positive. Therefore the flow enhances the mean axial transport of solute when $R_S \ll 1$.

After some calculation, it is found that

$$\mathscr{R} = \epsilon^2 \left[\tfrac{1}{2}h_0 + \frac{\alpha^6\sigma^2 \sinh\beta \sinh\bar{\beta}}{D\bar{D}} \sum_{n=1}^{\infty} \frac{h_n}{(\alpha^4\sigma^2 + n^4\pi^4)(\alpha^4 + n^4\pi^4)} \right.$$
$$\left. + \frac{\alpha^6\sigma^2 \sinh\beta \sinh\bar{\beta}}{D\bar{D}} \left(\frac{L^2 + Ll + l^2}{3} \right) \sum_{n=1}^{\infty} \frac{n^2\pi^2}{(\alpha^4\sigma^2 + n^4\pi^4)(\alpha^4 + n^4\pi^4)} \right] + O(\epsilon^4), \tag{4.17}$$

where

$$h_n = \frac{n^4\pi^4 - \alpha^4\sigma^2}{n^4\pi^4 + \alpha^4\sigma^2} - (L-l)\,\mathrm{Re}\left\{ \frac{\bar{\psi}_n^2}{2\psi_n} \coth\frac{\psi_n(L-l)}{2} \right\} - \frac{(L+l)^2}{(L-l)}\,\mathrm{Re}\left\{ \frac{\bar{\psi}_n^2}{2\psi_n} \tanh\frac{\psi_n(L-l)}{2} \right\}. \tag{4.18}$$

The first term in (4.17) is the mean relative increase in solute flux for an inviscid fluid, which arises from axial advection and diffusion of solute at the cross-sectionally averaged concentration. It is useful to see how the distribution of the cross-sectionally averaged concentration depends upon $\alpha\sigma^{\frac{1}{2}}(L-l)$, as plotted in figure 3. Note that when $\alpha\sigma^{\frac{1}{2}}(L-l) \gg 1$, the cross-sectionally averaged concentration is linear, except for boundary layers imposed by our choice of end conditions. It may be shown that no solution of the advection–diffusion equation (with any end conditions) exists that is linear in x, for a viscous fluid. The second term is a sum of similar contributions from each Fourier component of the concentration. We may approximate h_n for $n \geqslant 1$ by

$$h_n \sim \mathrm{Re}\left\{ \frac{\bar{\psi}_n^2}{\psi_n^2} \left(1 - \psi_n \frac{L^2 + l^2}{L-l} \right) \right\}, \tag{4.19}$$

because $L-l \gg 1$ and $|\psi_n| > n\pi$. Therefore, for a sufficiently long tube, each component of the sum in the second term will be much smaller than the corresponding component of the sum in the third term.

The third term in (4.17) is the result of transverse diffusion along the lateral

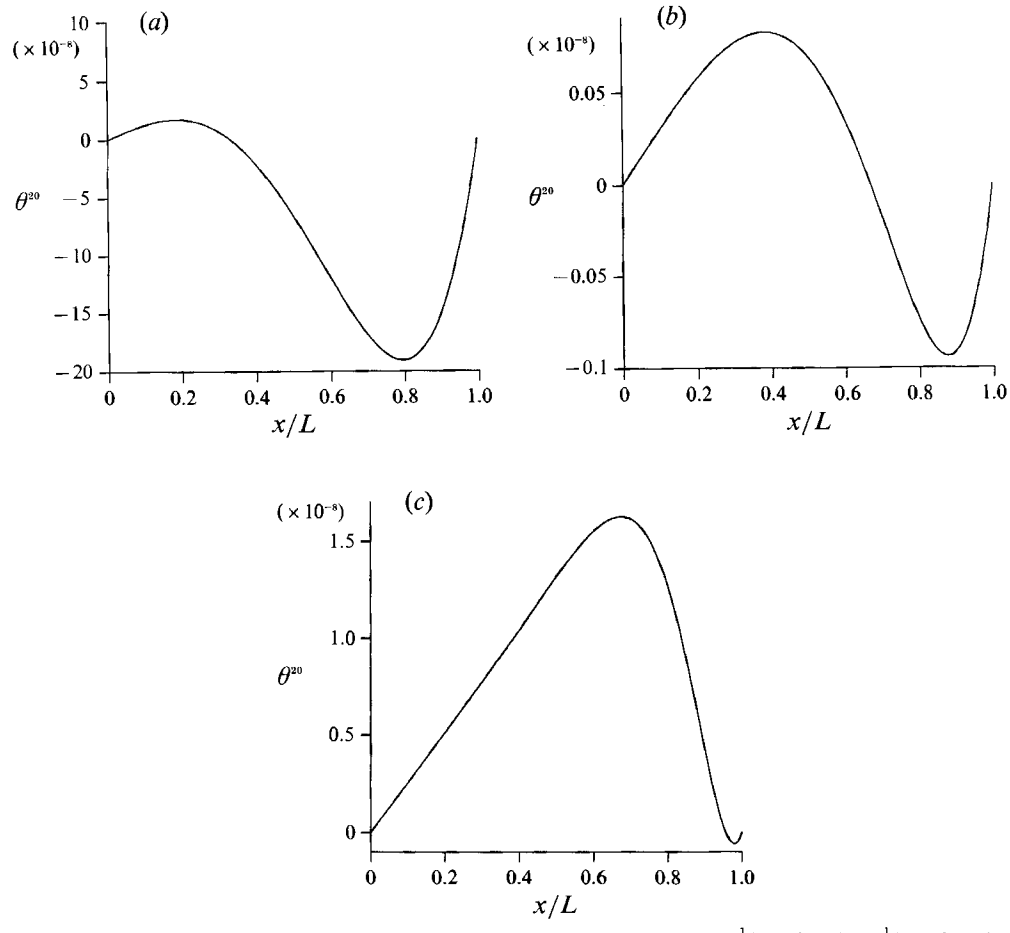

FIGURE 3. The variation in mean concentration with x, for various $\alpha\sigma^{\frac{1}{2}}(L-l)$: (*a*) $\alpha\sigma^{\frac{1}{2}}(L-l) = 0.1$; (*b*) 2.0; (*c*) 24.0. For all graphs $L = 12$, $l = -12$; only the half $0 < x < L$ is depicted.

concentration gradients produced by the shear. This part of the dispersion is similar to that found by Watson (1983) for a rigid channel. To see this, we need the result (obtained from (2.14)) that the leading-order pressure gradient in our problem is

$$\hat{p}_{\hat{x}} = -\epsilon\rho a_0 r\omega^2 |\cosh\beta/D| \operatorname{Re}\{\exp \mathrm{i}[t + \arg((1/D)\cosh\beta)]\}. \tag{4.20}$$

Watson found that for a flow with pressure gradient $\hat{p}_{\hat{x}} = -P\cos t$, the mean relative increase in solute flux is

$$\mathscr{R} = \frac{P^2}{2}\frac{\sigma^2}{\rho^2\nu\omega^3(\sigma^2-1)}\frac{\cosh\sqrt{2}\alpha-\cos\sqrt{2}\alpha}{\cosh\sqrt{2}\alpha+\cos\sqrt{2}\alpha} \times\left[\frac{\sinh\sqrt{2}\alpha-\sin\sqrt{2}\alpha}{\sqrt{2}\alpha(\cosh\sqrt{2}\alpha-\cos\sqrt{2}\alpha)} - \frac{\sinh\sqrt{2}\alpha\sigma^{\frac{1}{2}}-\sin\sqrt{2}\alpha\sigma^{\frac{1}{2}}}{\sqrt{2}\alpha\sigma^{\frac{1}{2}}(\cosh\sqrt{2}\alpha\sigma^{\frac{1}{2}}-\cos\sqrt{2}\alpha\sigma^{\frac{1}{2}})}\right] \tag{4.21}$$

which may be written as

$$\mathscr{R} = \frac{P^2\sigma^2\alpha^4}{\omega^3\rho^2\nu}\frac{\sinh\beta\sinh\bar{\beta}}{\cosh\beta\cosh\bar{\beta}}\sum_{n=1}^{\infty}\frac{n^2\pi^2}{(\alpha^4\sigma^2+n^4\pi^4)(\alpha^4+n^4\pi^4)}. \tag{4.22}$$

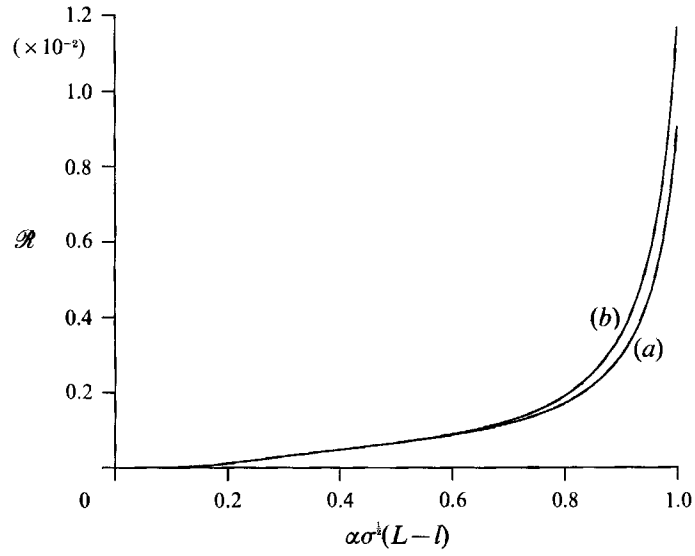

FIGURE 4. The variation in $\mathscr{R}$ with $\alpha\sigma^{\frac{1}{2}}(L-l)$: (*a*) $L = 12$, $l = -12$; (*b*) $L = 16$, $l = -8$. For both graphs $\epsilon = 0.02$, $\sigma = 1.0$.

In Watson's problem, the pressure gradient is independent of x, whereas (4.20) is linear in x. However, if we substitute the longitudinally averaged square of the pressure gradient amplitude,

$$\frac{2}{L-l}\int_{x=l}^{L} \langle \hat{p}_{\hat{x}}^2 \rangle \, \mathrm{d}x = \epsilon^2\rho^2 a_0^2\omega^4 \frac{\cosh\beta\cosh\bar{\beta}}{D\bar{D}}\frac{(L^2+Ll+l^2)}{3}, \tag{4.23}$$

into Watson's result, in place of his P^2, we obtain the third term in (4.17). It is not surprising that the average square pressure gradient should be used, for net conservation of solute over a period requires that $\mathscr{R}$ be independent of x. Thus, for a sufficiently long tube (i.e. one for which $\pi^2(L^3-l^3) \gg \alpha\sigma^{\frac{1}{2}}(L-l)^2$), the dispersion in a viscous fluid in a channel with oscillating walls is approximately the sum of that in an inviscid fluid and that produced in a viscous fluid in a rigid channel when the longitudinal average square pressure gradient is (4.23). The terms contributing to $\mathscr{R}$ are summed without apparent interaction, but we have calculated $\mathscr{R}$ only to leading order in ϵ; it is likely that interaction between terms would contribute to higher-order corrections. $\mathscr{R}$ is plotted against $\alpha\sigma^{\frac{1}{2}}(L-l)$ (for two sets of values of L, l, with the same value of $L-l$) in figure 4.

A similar calculation for a cylindrical pipe of radius $\hat{a}(\hat{t})$ gives the result

$$\mathscr{R} = \epsilon^2\left[\tfrac{1}{2}+2h_0' + \frac{8\alpha^6\sigma^2 I_1(\beta)I_1(\bar{\beta})}{D'\bar{D}'}\sum_{n=1}^{\infty}\frac{h_n'}{(\alpha^4\sigma^2+\lambda_n^4)(\alpha^4+\lambda_n^4)}\right.$$
$$\left. + \frac{8\alpha^6\sigma^2 I_1(\beta)I_1(\bar{\beta})}{D'\bar{D}'}\left(\frac{L^2+Ll+l^2}{3}\right)\sum_{n=1}^{\infty}\frac{\lambda_n^2}{(\alpha^4\sigma^2+\lambda_n^4)(\alpha^4+\lambda_n^4)}\right] + O(\epsilon^4), \tag{4.24}$$

where

$$h_n' = \frac{\lambda_n^4-\alpha^4\sigma^2}{\lambda_n^4+\alpha^4\sigma^2} - (L-l)\,\mathrm{Re}\left\{\frac{\bar{\psi}_n'^2}{2\psi_n'}\coth\frac{\psi_n'(L-l)}{2}\right\} - \frac{(L+l)^2}{L-l}\,\mathrm{Re}\left\{\frac{\bar{\psi}_n'^2}{2\psi_n'}\tanh\frac{\psi_n'(L-l)}{2}\right\}, \tag{4.25}$$

λ_n is the nth non-negative zero of the first-order Bessel function $J_1(\lambda)$ ($\lambda_0 = 0$), I_m is the modified Bessel function of order m, $D' = I_0(\beta) - 2I_1(\beta)$, and $\psi' = (\lambda_n^2 + \beta^2\sigma)^{\frac{1}{2}}$.

The first term in (4.24) arises because the mean pipe area is $\pi\langle\hat{a}^2(\hat{t})\rangle = \pi a_0^2(1+\frac{1}{2}\epsilon^2)$, so that when there is wall motion, diffusion due to the leading-order concentration gradient ($\theta_x^{00} = 1$) is a factor $\frac{1}{2}\epsilon^2$ greater than when there is no wall motion. By contrast, the mean width of a two-dimensional channel is $2\langle\hat{a}(\hat{t})\rangle = 2a_0$, so the diffusion due to θ_x^{00} is independent of the wall motion. The remaining terms in (4.24) correspond to those in (4.17), which have been discussed above.

Although we have omitted explicit expressions for θ^{20} and higher-order terms, these have been calculated, and it is found that the condition that the series expansion be asymptotic is that $P_S = \epsilon^2\alpha^2\sigma(L-l)^2 \ll 1$. In the next section, we study the singular problem which arises when this condition is not satisfied.

5. Dispersion in a channel: large mean Péclet number

In the parameter regime examined so far, we have found that the solute distribution satisfies $\theta(x, \eta, t) = x[1 + O(\epsilon)]$, where the wall-driven flow determines the correction terms. As a result, $\mathscr{R}$ is of order ϵ^2. When $R_S \gg 1$ however, we find the concentration is not approximated to leading order by $\theta(x, \eta, t) \sim x$.

Following Secomb, we write $\alpha^2 = N^2\epsilon^{-2(1+c)}$, where $c > 0$, so that $R_S = N^2\epsilon^{-2c} \to \infty$ as $\epsilon \to 0$. For ease of calculation, we examine only the symmetric case, with the origin located at the midpoint of the channel. However, the results will be little altered in the case when the origin is not in the channel centre. It proves to be convenient to use the rescaled concentration $\tilde{\theta} = \theta/L$. The advection–diffusion equation in non-dimensional variables is

$$\tilde{\theta}_t - x\left(\frac{\dot{a}}{a} + a^2F_\eta\right)\tilde{\theta}_x + a^2F\tilde{\theta}_\eta = \frac{\epsilon^{2(1+c)}}{N^2\sigma}(\tilde{\theta}_{xx} + \tilde{\theta}_{\eta\eta}/a^2), \tag{5.1}$$

where the function $F(\eta, t)$ is defined by (2.15). We may neglect diffusion, provided that the right-hand side of (5.1) remains much smaller than the left-hand side, i.e. that neither $\tilde{\theta}_{xx}$ nor $\tilde{\theta}_{\eta\eta}$ becomes too large. Therefore, let us see how the concentration evolves (to leading order) when diffusion is neglected. We solve the initial value problem

$$\tilde{\theta}_t - x(\dot{a}/a + a^2F_\eta)\tilde{\theta}_x + a^2F\tilde{\theta}_\eta = 0, \tag{5.2}$$

$$\tilde{\theta}(x, \eta, -\pi) = \begin{cases} x/L & \text{when } |x| < L; \\ \operatorname{sgn}(x) & \text{when } |x| > L. \end{cases} \tag{5.3}$$

(The initial time $t = -\pi$ corresponds to the channel having minimum width.) There is a gradient discontinuity in the initial condition which is advected with the fluid in the absence of diffusion; diffusion would smooth the discontinuity, but the concentration profile would be only slightly modified during the first few oscillation cycles.

Equations (5.1) and (5.2) may be solved using the method of characteristics, using (2.16) to substitute for F within the core, so that, neglecting terms of $O(\epsilon^4 t)$,

$$\tilde{\theta}(x, \eta, t) \approx \frac{a(t)\,x}{a(-\pi)\,L}\left[\cosh\frac{3\epsilon^2 t}{4} - \cos\pi\eta\sinh\frac{3\epsilon^2 t}{4}\right], \tag{5.4a}$$

provided that the modulus of the right-hand side of (5.4a) is less than 1. Otherwise,

$$\tilde{\theta}(x, \eta, t) = \operatorname{sgn}(x). \tag{5.4b}$$

Contours of equal concentration are shown in figure 5, for $\epsilon^2 t = O(1)$ and for $\epsilon^2 t \gg 1$.

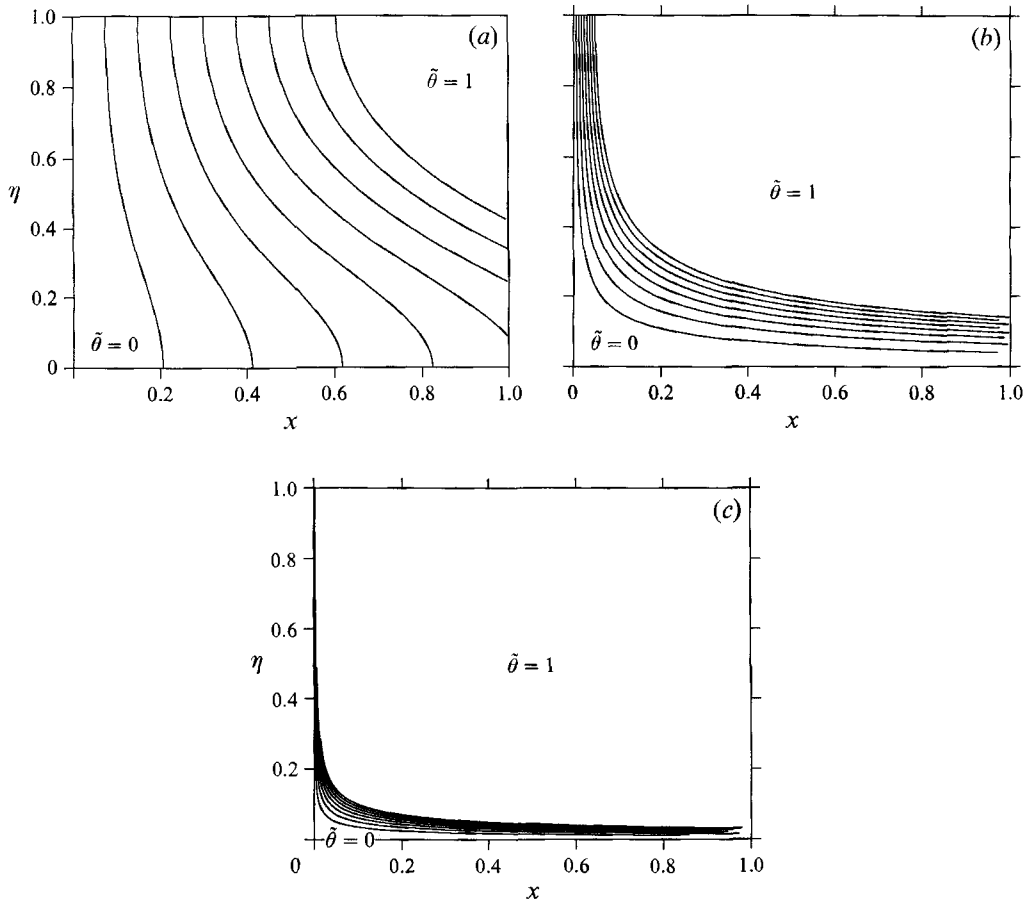

FIGURE 5. The long-time evolution of (equally spaced) concentration contours (only the quadrant $0 < x < L$, $0 < \eta < 1$ is shown. (*a*) $\epsilon^2 t = \frac{2}{3}$; (*b*) 4; (*c*) 8.

There is very little change in the calculated distribution from one cycle to the next, but we see that eventually the steady streaming causes large regions of uniform concentration to be set up within the core, separated by zones in which the concentration gradients are large, close to $x = 0$ and $\eta = 0$. In these zones, the assumption that diffusion is negligible has become invalid. We therefore undertake a full analysis of the $O(1)$ solute distribution, taking account of diffusion, using the above results as a guide.

They lead us to expect that an initially linear concentration profile will, over many cycles, be advected by the steady streaming until large concentration gradients are set up. Diffusion along these large gradients results, so that equilibrium is reached, at least as far as the $O(1)$ steady term is concerned. (There will also be an oscillatory variation in the concentration at $O(\epsilon)$, but we neglect this and higher-order corrections, as our main purpose is to determine $\mathscr{R}$.) The regions in which the equilibrium concentration gradient will be large appear (from figure 5) to be a neighbourhood of $x = 0$ (where the axial velocity vanishes) and a neighbourhood of the centreline $\eta = 0$. We must also investigate the Stokes layers on the oscillating walls. Away from these regions, in $x > 0$, the concentration is equal to that in the tank, i.e. $\tilde{\theta} = 1$. Similarly, for $x < 0$, the concentration is $\tilde{\theta} = -1$ away from the regions where the concentration gradient is

large. These conclusions will assist us in the analysis of the equilibrium distribution of solute.

We must solve the advection–diffusion equation (5.1) subject to the boundary conditions at the walls

$$\tilde{\theta}_\eta = 0 \quad \text{at} \quad \eta = \pm 1 \tag{5.5}$$

and suitable end conditions. From figure 5, we anticipate that the equilibrium solute distribution will be uniform in the region of $x = L$, except in the neighbourhood of $\eta = 0$ (and possibly the Stokes layers). Therefore, provided that the region of uniform concentration extends into the channel for a distance greater than a stroke length (which is $O(\epsilon L)$ channel widths), the concentration at $x = L$ will be $\tilde{\theta} = 1$ independently of time, except perhaps near $\eta = 0$ or $\eta = 1$, as mentioned above.

We now use the symmetries of the problem ($\tilde{\theta}$ is odd in x, even in η) to restrict attention to the quadrant $x > 0$, $\eta > 0$. The Stokes layer at $\eta = 1$ is of thickness $O(\epsilon^{1+c})$, so we introduce the Stokes-layer variable $\zeta = \epsilon^{-(1+c)}(1-\eta)$. The left-hand side of (5.1) is $O(\epsilon)$, so in the Stokes layer at $\eta = 1$ the leading-order part of the concentration satisfies

$$\tilde{\theta}^{00}_{\zeta\zeta} = 0 \quad \text{subject to} \quad \tilde{\theta}^{00}_{\zeta} = 0 \quad \text{at} \quad \zeta = 0, \tag{5.6}$$

provided that $\epsilon^{2(1+c)}\tilde{\theta}^{00}_{xx} \ll 1$. We will assume that this last condition holds, and check later for consistency. Therefore, $\tilde{\theta}^{00}$ is a function of x only and so $\tilde{\theta}^{00}_\eta \equiv 0$ throughout the Stokes layer. As a result, the boundary condition on $\tilde{\theta}^{00}$ within the core is

$$\tilde{\theta}^{00}_\eta \to 0 \quad \text{as} \quad \eta \to 1. \tag{5.7}$$

Within the core, we use (2.15) and (2.16) to obtain the advection–diffusion equation

$$\tilde{\theta}_t + \left(-\frac{a_t}{a} + \tfrac{3}{4}\epsilon^2 a^2 \cos \pi\eta\right) x\tilde{\theta}_x - \frac{3}{4\pi}\epsilon^2 a^2 \sin \pi\eta\, \tilde{\theta}_\eta = \frac{\epsilon^{2(1+c)}}{N^2\sigma}\left(\frac{1}{a^2}\tilde{\theta}_{\eta\eta} + \tilde{\theta}_{xx}\right). \tag{5.8}$$

(Terms in F which are $O(\epsilon^4)$ have been omitted from (5.8); they do not contribute to the leading-order steady concentration profile.) First, we assume that the right-hand side of (5.8) can be neglected, i.e. $\epsilon^{2c}(\tilde{\theta}^{00}_{\eta\eta} + \tilde{\theta}^{00}_{xx}) \ll 1$. Substituting a series expansion for $\tilde{\theta}$, we obtain at $O(\epsilon)$

$$\mathrm{i}\tilde{\theta}^{11} - \mathrm{i}x\tilde{\theta}^{00}_x = 0, \tag{5.9}$$

and the steady part at $O(\epsilon^2)$

$$\tfrac{3}{4}x \cos \pi\eta \tilde{\theta}^{00}_x + \tfrac{1}{2}\,\mathrm{Re}\{\mathrm{i}x\tilde{\theta}^{11}_x\} - \frac{3}{4\pi}\sin \pi\eta \tilde{\theta}^{00}_\eta = 0. \tag{5.10}$$

$\tilde{\theta}^{00}$ is real, so $\tilde{\theta}^{11}$ is also real, from (5.9). Hence the second term in (5.10) is zero. Therefore, the general solution of (5.10) subject to the matching condition (5.7) is

$$\tilde{\theta}^{00} = f(x \sin \pi\eta) \quad \text{where} \quad f'(0) = 0. \tag{5.11}$$

The function f is to be determined from end conditions.

In physical terms, $\tilde{\theta}^{00}$ is constant on the streamlines of the steady-streaming flow. The steady streaming is directed into the channel at $x = L$, for $\eta > \frac{1}{2}$, carrying fluid at the end concentration $\tilde{\theta}^{00} = 1$. Therefore

$$f(L \sin \pi\eta) = 1 \quad \text{for} \quad 1 > \eta > \tfrac{1}{2}, \tag{5.12}$$

and so $f \equiv 1$. Thus, in the region in the quadrant $x > 0$, $\eta > 0$ for which the right-hand side of (5.8) remains negligible, the leading-order concentration is

$$\tilde{\theta}^{00} = 1. \tag{5.13}$$

This solution breaks down close to $x = 0$, where the concentration is required to be zero because $\tilde{\theta}$ is odd in x. Comparison of terms in (5.8) indicates the presence of a boundary layer at $x = 0$, of thickness $O(\epsilon^c)$, in which the concentration changes rapidly from $\tilde{\theta}^{00} = 0$ to $\tilde{\theta}^{00} = 1$ as x increases. Furthermore, the steady streaming advects the large concentration gradients around the corner (near the stagnation point $x = 0$, $\eta = 0$) into the region $\eta = O(\epsilon^c)$. Thus a 'tongue' of fluid with concentration $\tilde{\theta}^{00} < 1$ is advected along the centre of the channel; advection of lower-concentration fluid also caused such a tongue in the initial value problem considered earlier, whose long-time solution is depicted in figure 5.

To analyse the boundary layer at $x = 0$, we introduce the scaled coordinate $\xi = \frac{1}{2}x\epsilon^{-c}(3\sigma)^{\frac{1}{2}}N = \frac{1}{2}x(3R_S\sigma)^{\frac{1}{3}}$. This scaling arises because the (Lagrangian) steady streaming tends to increase the time-averaged axial concentration gradient at $x = 0$, a process which is balanced by longitudinal diffusion within the boundary layer. From (5.8), the concentration satisfies

$$\tilde{\theta}_t + \left(-\frac{a_t}{a} + \tfrac{3}{4}\epsilon^2 a^2 \cos \pi\eta\right)\xi\tilde{\theta}_\xi - \frac{3}{4\pi}\epsilon^2 a^2 \sin \pi\eta\tilde{\theta}_\eta = \tfrac{3}{4}\epsilon^2\tilde{\theta}_{\xi\xi} + \frac{\epsilon^{2(1+c)}}{N^2\sigma a^2}\tilde{\theta}_{\eta\eta}, \tag{5.14}$$

within the boundary layer close to $x = 0$. Provided that $\epsilon^{2c}\tilde{\theta}^{00}_{\eta\eta} \ll 1$, the leading-order concentration is determined from the $O(\epsilon)$ equation

$$i\tilde{\theta}^{11} - i\xi\tilde{\theta}^{00}_\xi = 0 \tag{5.15}$$

and the $O(\epsilon^2)$ steady equation

$$\tfrac{3}{4}\xi \cos \pi\eta\tilde{\theta}^{00}_\xi + \tfrac{1}{2}\mathrm{Re}\{i\xi\tilde{\theta}^{11}_\xi\} - (3/4\pi)\sin \pi\eta\tilde{\theta}^{00}_\eta = \tfrac{3}{4}\tilde{\theta}^{00}_{\xi\xi}. \tag{5.16}$$

The second term on the left-hand side of (5.16) vanishes as before, because $\tilde{\theta}^{11}$ is real, so we must solve

$$\xi \cos \pi\eta\tilde{\theta}^{00}_\xi - (1/\pi)\sin \pi\eta\tilde{\theta}^{00}_\eta = \tilde{\theta}^{00}_{\xi\xi}, \tag{5.17}$$

subject to the conditions

$$\tilde{\theta}^{00} = 0 \quad \text{at} \quad \xi = 0; \qquad \tilde{\theta}^{00} \to 1 \quad \text{as} \quad \xi \to \infty \tag{5.18}$$

and the matching condition (5.7). The change of variables

$$r = \xi \sin \pi\eta; \quad s = 1 + \cos \pi\eta \tag{5.19}$$

reduces (5.17) to the one-dimensional diffusion equation,

$$\tilde{\theta}^{00}_s = \tilde{\theta}^{00}_{rr}, \tag{5.20}$$

and the solution is

$$\tilde{\theta}^{00} = \mathrm{erf}\left(\frac{\xi}{\sqrt{2}}\sin\frac{\pi\eta}{2}\right). \tag{5.21}$$

Clearly the matching condition (5.7) is satisfied by the solution (5.21). In addition, $\tilde{\theta}^{00}_{\xi\xi} = O(1)$ in the neighbourhood of $\eta = 1$, so $\epsilon^{2(1+c)}\tilde{\theta}^{00}_{xx} = O(\epsilon^2) \ll 1$ in this region, and the assumption leading to (5.6) is justified; the solution (5.21) holds within the Stokes layer near $\xi = 0$, $\eta = 1$.

The approximation on which this solution is based becomes invalid when $\epsilon^{2c}\tilde{\theta}^{00}_{\eta\eta}$ becomes of order unity. This happens when $\eta = O(\epsilon^c)$ and $\xi = O(\epsilon^{-c})$, i.e. just outside the boundary layer at $x = 0$, in the tongue centred on $\eta = 0$. Close to the stagnation point $x = 0$, $\eta = 0$, the solute is advected around the corner. To see this, note that the stream-lines of the steady-streaming flow in the neighbourhood of the stagnation point satisfy $x\eta = \text{constant}$, to a first approximation. From (5.21) we see that, within the

neighbourhood, $\tilde{\theta}^{00}$ is proportional to $x\eta$, again to a first approximation. Therefore $\tilde{\theta}^{00}$ is constant on the streamlines, which are symmetric under reflection in the line $x = \eta$. Hence the solute is advected around the corner without change of profile. This produces a concentration gradient discontinuity at $\eta = 0$, which will be smoothed by diffusion. However, the effect of this smoothing is only $O(\epsilon^c)$ in the boundary layer adjoining $x = 0$. The diffusive smoothing produces an $O(1)$ change in $\tilde{\theta}^{00}$ only when $x \geqslant O(1)$. Therefore we will use the boundary-layer solution to give the conditions as $x \to 0$ on the solution in the tongue.

Advection of a boundary layer by steady streaming has been analysed previously. Lyne (1971), for example, studied unsteady flow in a curved pipe when $R_S \gg 1$, and found that centrifugal forces produce a steady secondary flow directed from the outer wall to the inner wall of the pipe; thin boundary layers are attached to the pipe wall, in which the vorticity gradients are confined. The uniform vorticity steady streaming in the core advects non-uniform vorticity from the boundary layer through 90° into a tongue on the plane of symmetry of the pipe.

To formulate the problem in the tongue, we introduce the scaled transverse coordinate $\gamma = \frac{1}{2}\eta\epsilon^{-c}(3\sigma)^{\frac{1}{2}}N$. Substituting this into the advection–diffusion equation (5.8) and taking leading-order approximations to the trigonometric functions results in the equation for the concentration in the tongue

$$x\tilde{\theta}^{00}_x - \gamma\tilde{\theta}^{00}_\gamma = \tilde{\theta}^{00}_{\gamma\gamma} + (4\epsilon^{2c}/3N^2\sigma)\,\tilde{\theta}^{00}_{xx}, \tag{5.22}$$

where the $O(\epsilon)$ equation has been used to eliminate a term from the steady $O(\epsilon^2)$ equation, as before. The second term on the right-hand side of (5.22) is small for $x \gg \epsilon^c$ and may be neglected. If the matching between the boundary-layer solution (5.21) and the solution of (5.22) takes place at $x = \chi$, where $\epsilon^c \ll \chi \ll 1$, the matching condition is

$$\tilde{\theta}^{00}(\chi, \gamma) = \operatorname{erf}[(\pi/\sqrt{8})\,\chi|\gamma|]. \tag{5.23}$$

We consider the whole tongue, which is symmetric about the line $\eta = 0$; the symmetry condition is

$$\tilde{\theta}^{00}_\gamma(x, 0) = 0 \quad \text{for} \quad x > \chi. \tag{5.24}$$

The matching condition to the solution (5.13) is

$$\tilde{\theta}^{00}(x, \gamma) \to 1 \quad \text{as} \quad \gamma \to \infty \quad \text{for} \quad x > \chi. \tag{5.25}$$

By introducing the coordinates $p = \frac{1}{2}x^2$, $q = x\gamma$, equation (5.22) may be transformed to the diffusion equation

$$\tilde{\theta}^{00}_p = \tilde{\theta}^{00}_{qq}. \tag{5.26}$$

The conditions (5.23)–(5.25) transform to

$$\tilde{\theta}^{00}(\tfrac{1}{2}\chi^2, q) = \operatorname{erf}[(\pi/\sqrt{8})\,|q|], \tag{5.27}$$

$$\tilde{\theta}^{00}_q(p, 0) = 0 \quad \text{for} \quad p > \tfrac{1}{2}\chi^2, \tag{5.28}$$

$$\tilde{\theta}^{00}(p, q) \to 1 \quad \text{as} \quad q/\sqrt{2p} \to \infty \quad \text{for} \quad p > \tfrac{1}{2}\chi^2. \tag{5.29}$$

The solution of (5.26)–(5.29) is

$$\tilde{\theta}^{00}(p, q) = \left(\frac{2}{\pi^3(p - \frac{1}{2}\chi^2)}\right)^{\frac{1}{2}} \int_0^\infty \operatorname{erf}(w) \left\{ \exp\left[-\left(\frac{\sqrt{2}w}{\pi(p - \frac{1}{2}\chi^2)^{\frac{1}{2}}} - \frac{q}{2(p - \frac{1}{2}\chi^2)^{\frac{1}{2}}} \right)^2 \right] + \exp\left[-\left(\frac{\sqrt{2}w}{\pi(p - \frac{1}{2}\chi^2)^{\frac{1}{2}}} + \frac{q}{2(p - \frac{1}{2}\chi^2)^{\frac{1}{2}}} \right)^2 \right] \right\} \mathrm{d}w. \tag{5.30}$$

Reverting to (x, γ) coordinates, we obtain

$$\tilde{\theta}^{00}(x,\gamma) = \left(\frac{4}{\pi^3(x^2-\chi^2)}\right)^{\frac{1}{2}} \int_0^\infty \operatorname{erf}(w) \left\{ \exp\left[-\left(\frac{2w}{\pi(x^2-\chi^2)^{\frac{1}{2}}} - \frac{\gamma}{2(1-\chi^2/x^2)^{\frac{1}{2}}} \right)^2 \right] + \exp\left[-\left(\frac{2w}{\pi(x^2-\chi^2)^{\frac{1}{2}}} + \frac{\gamma}{(2(1-\chi^2/x^2))^{\frac{1}{2}}} \right)^2 \right] \right\} \mathrm{d}w. \quad (5.31)$$

When $x \gg \chi$, (5.31) may be approximated by

$$\tilde{\theta}^{00}(x,\gamma) = \frac{2}{\pi^{\frac{3}{2}} x} \int_0^\infty \operatorname{erf}(w) \left\{ \exp\left[-\left(\frac{2w}{\pi x} - \frac{\gamma}{\sqrt{2}} \right)^2 \right] + \exp\left[-\left(\frac{2w}{\pi x} + \frac{\gamma}{\sqrt{2}} \right)^2 \right] \right\} \mathrm{d}w. \quad (5.32)$$

Equation (5.32) describes the solute distribution in the tongue for $x \gg \epsilon^c$. A reasonable idea of the concentration may be obtained by evaluating the integral at $\gamma = 0$, where the concentration is minimized with respect to γ. This leads to

$$\tilde{\theta}^{00}(x,0) = 1 - (2/\pi)\tan^{-1}(2/\pi x). \quad (5.33)$$

The second term decays algebraically (like x^{-1}) as x becomes large and, for a sufficiently long channel, the concentration in the tongue is close to that in the tank at $x = L$. In a cylindrical pipe, the concentration defect in the tongue falls off exponentially with x.

We may evaluate the relative increase in solute flux across the cross-section $x = 0$ using (5.21):

$$\mathscr{R} = \int_{\eta=0}^{1} \theta_x^{00}(0,\eta)\,\mathrm{d}\eta - 1 + O(\epsilon)$$

$$= \frac{\sqrt{6}}{\pi^{\frac{3}{2}}} \epsilon L \alpha \sigma^{\frac{1}{2}} - 1 + O(\epsilon) = O(P_S^{\frac{1}{2}}). \quad (5.34)$$

The corresponding result for a cylindrical pipe is

$$\mathscr{R} = \frac{4\sqrt{6}}{\pi^{\frac{3}{2}}} \epsilon L \alpha \sigma^{\frac{1}{2}} - 1 + O(\epsilon). \quad (5.35)$$

Clearly, $\mathscr{R}$ increases without limit as P_S increases. The reason for this is the increasingly steep mean axial concentration gradient close to $x = 0$, which is caused by advection with the steady streaming, resulting in an enhanced diffusion across the plane $x = 0$. The tongue on $\eta = 0$ makes a negligible contribution to the solute flux across $x = 0$.

It has been convenient to take $l = -L$ and use the symmetries of the problem to find the solution. However, we see that the axial concentration boundary layer and the tongue on the centreline are the only places where the concentration differs from that at the channel ends. Therefore it may be concluded that, provided l, L are located well away from $x = 0$, there will be an axial boundary layer in the neighbourhood of $x = 0$ and a tongue on the centreline, irrespective of the precise location of l and L. Except for the tongue, it is as if the end conditions have been brought into the channel by steady streaming, so that they determine the concentration at either side of the central layer. If $l \neq -L$, we may change variables to reduce the problem to the symmetric case: let the rescaled concentration be $\tilde{\theta} = 2/(L-l)(\theta - \frac{1}{2}(L+l))$. (This rescaling is a slight generalization of that used in the symmetric case.) Then all of the working goes through as before, except that (5.34) is replaced by the more general

$$\mathscr{R} = \frac{\sqrt{3}}{\pi(2\pi)^{\frac{1}{2}}} \epsilon (L-l)\,\alpha \sigma^{\frac{1}{2}} - 1 + O(\epsilon). \quad (5.36)$$

For a cylindrical pipe, (5.35) is replaced by

$$\mathscr{R} = \frac{2\sqrt{6}}{\pi^{\frac{3}{2}}}\epsilon(L-l)\alpha\sigma^{\frac{1}{2}} - 1 + O(\epsilon). \tag{5.37}$$

Finally, let us consider the problem when $P_S \gg 1$, but $R_S = O(1)$. For $R_S \gg 1$ we have found that, with the axial steady streaming directed into the channel in the part of the core adjacent to the walls and out of the channel elsewhere, an axial concentration boundary layer develops close to $x = 0$. The boundary-layer thickness (relative to the channel length) is $O(P_S^{-\frac{1}{2}})$. Secomb (1978) computed the steady streaming when $R_S = O(1)$; the results are shown in figure 6 of his paper. He found that the profile of the steady-streaming flow when $R_S = O(1)$ is similar in shape to (and of the same order of magnitude as) the case $R_S \gg 1$. The axial flow is again directed into the channel adjacent to the walls and out of the channel elsewhere.

Therefore, although it has been convenient (from an algebraic point of view) to study the case $R_S \gg 1$, we expect that the same physical processes operate when $R_S = O(1)$, provided that $P_S \gg 1$. Advection is the dominant mechanism of transport in most of the channel, but there is a concentration boundary layer of thickness $O(P_S^{-\frac{1}{2}})$ in the region where the axial velocity vanishes. Transport is markedly enhanced by the wall motion, for the relative increase in solute flux across $x = 0$ is $\mathscr{R} = O(P_S^{\frac{1}{2}})$.

6. Application to high-frequency ventilation (HFV)

We have shown that transverse oscillation of the walls of a straight channel (or pipe of circular cross-section) induces a flow which augments the mean axial solute transport. In particular, when the fluid is viscous and $R_S \gg 1$, the transport is enhanced by a factor $O(P_S^{\frac{1}{2}}) \gg 1$. Solute is transported within the channel mainly by advection, which dominates diffusion over most of the channel. The steady streaming draws solute from the tanks towards the region where the axial advection vanishes, resulting in a thin boundary layer in which the axial concentration gradient is large. Diffusion down the large concentration gradient produces a large solute flux. The argument presented at the end of §5 indicates that the same physical processes operate for $R_S = O(1)$, provided that $P_S \gg 1$.

When $P_S \ll 1$, the analysis of §4 indicates that the mean increase in axial solute flux is $O(\epsilon^2) \ll 1$. Diffusion dominates advection in this parameter range, so that, to leading order in ϵ, the concentration is unchanged by the wall motion. Advection produces an oscillatory change in the concentration of $O(\epsilon)$, and a mean change of $O(\epsilon^2)$. These changes lead to an $O(\epsilon^2)$ enhancement in mean solute flux.

The model problem was motivated by the need to understand the mechanisms responsible for gas transport in the human lung during HFV. We now examine the predictions of the model problem for the parameter range relevant to the human lung. A typical frequency is 15 Hz; a typical tidal volume is 50 ml. Hughes, Hoppin & Mead (1972) inflated and deflated excised dog lungs, and found that the percentage change in airway diameter (and length) is proportional to the cube root of the percentage change in lung volume, with little dependence upon the airway generation. Given that the total volume of a human lung (at 75% of total lung capacity) is 4800 ml (Weibel 1963), we will therefore assume that the airway diameter varies by a factor $(\frac{50}{4800})^{\frac{1}{3}}$ during a cycle; this means that the relative amplitude of the wall oscillation is $\epsilon \approx 0.1$. We consider the transport of oxygen in the airways (the transport of carbon dioxide may be considered similarly). The molecular diffusivity of oxygen in dry air at 20 °C is

$\kappa = 0.18$ cm^2/s; the kinematic viscosity of dry air at 20 °C is $\nu = 0.15$ cm^2/s. Therefore the Schmidt number is $\sigma \approx 0.83$.

Let a_0 and $\hat{L} = a_0 L$ be the airway radius and length (in cm) respectively. Then the steady-streaming Péclet number is

$$P_S = \epsilon^2 \alpha^2 \sigma L^2 = \epsilon^2 \hat{L}^2 \omega / \kappa \approx 5.24 \hat{L}^2 \tag{6.1}$$

and the steady-streaming Reynolds number is

$$R_S = \epsilon^2 \alpha^2 = \epsilon^2 a_0^2 \omega / \nu \approx 6.28 a_0^2. \tag{6.2}$$

We use the measurements made by Weibel (1963) (incorporated into his symmetric lung model) to determine the range of values of R_S and P_S in the human lung.

The trachea (generation 0) is the largest airway, with radius $a_0 = 0.9$ cm and length $\hat{L} = 12.0$ cm. Clearly, $P_S \gg R_S > 1$ for the trachea, so the parameter regime is that studied in §5, but there is no location where the flow rate is zero, so if the present mechanism were the only one giving rise to enhanced mixing, all gas would be advected by the steady streaming through to the smaller airways. The same arguments applies in those successive generations for which $P_S \gg 1$. When $P_S = O(1)$, diffusion and advection by steady streaming are of the same order of magnitude. $P_S \approx 3.03$ for airways of generation 7 in the Weibel model; P_S is larger for the larger airways and smaller for the smaller airways. Therefore, the mean oxygen concentration would be expected to be uniform in the larger airways, but would fall in the smaller airways, because the steady streaming is not sufficiently strong to advect fresh gas into these airways faster than diffusion transports the oxygen to the alveoli. Nevertheless, if we suppose that the concentration is uniform in the generations 1–7, we find that the steady streaming would, if there were no other mechanism, transport fresh gas a distance of 23.42 cm, which is 86% of the total path length from the trachea to the alveoli in Weibel's model lung. This result may be extended to more general flows for which the Péclet number based upon the longitudinal component of the steady streaming is large in the largest airways, because the steady streaming advects fresh gas towards the periphery of the lung.

In the smaller airways, there are other mechanisms acting to enhance longitudinal mixing in the lung. The shear dispersion analysed for pressure-driven oscillatory flow in a straight tube by, for example, Watson (1983) is one example. For large α and $\sigma = 1$, Watson's theory predicts an enhanced transport rate, $\mathscr{R}$, proportional to $\kappa(L_S/a)^2 \alpha$, where L_S is the mean axial displacement of a fluid element during the oscillation. One can regard dispersion in an airway in which the concentration is non-uniform (i.e. generation 8 and smaller) as being due to a pressure-driven flow superimposed on the flow caused by the wall motion. Hydon (1991) found that the contribution to dispersion due to the pressure-driven part of the flow (determined by Watson) is larger in magnitude than the contribution due to the wall motion. However, the two mechanisms are not purely additive, and the eventual enhancement of dispersion depends crucially on the phase relation between the wall motion and the pressure gradient (cf. Dragon & Grotberg 1991).

Furthermore, the airways are not long straight pipes, but suffer repeated bifurcations. These can generate additional steady-streaming effects (Haselton & Scherer 1982), and significantly influence the cross-stream mixing because of the secondary motions that are set up (Schroter & Sudlow 1969; Shapiro & Kamm 1989). There may also be turbulence in the larger airways, generated either by the airway geometry or by the mechanical method of forcing the oscillatory flow (e.g. a jet ventilator: Kamm, Bullister & Keramidas 1986). In general, mechanisms such as these

which enhance transverse mixing tend to diminish the longitudinal dispersion (an exception occurs when there is resonance between the period of the axial oscillation and the secondary recycling time: Pedley & Kamm 1988; Sharp *et al.* 1991). The consequence would be to increase the importance of steady streaming. However, it is clear that the significance of the present contribution is more in the identification of a novel mechanism for the enhancement of longitudinal mass transport in oscillatory flow than in explaining standard experiments on HFV.

Finally, it is worth noting that there is at least one other problem arising in nature to which the present work (or a slight modification of it) may be applicable: insect respiration. Weis-Fogh (1964) studied diffusion in insect wing muscle, which consumes oxygen at a rate which is higher than any other muscle. Oxygen is supplied to this muscle by a long straight primary trachea, which has a number of secondary trachea branching off it (mainly at right angles). Weis-Fogh calculated steady-state diffusion rates in the wing muscle of various insects, but concluded that in at least one insect, the giant belostomid bug *Lethocerus uhleri*, the dimensions of the wing muscle are inconsistent with the calculated rate of oxygen transport by diffusion. The walls of the tracheae are surrounded by muscle fibres, which contract and relax at high frequency during flight. It is therefore to be expected that the wall-driven flow analysed by Secomb (1978) will occur in the tracheae and, if P_S is sufficiently large, fresh gas may be brought into the airways by steady streaming.

During the course of this work P.E.H. was supported by an SERC CASE studentship in the Department of Applied Mathematics and Theoretical Physics, Cambridge University, in conjunction with Addenbrookes Hospital. We are grateful to the referees for their comments and suggestions.

REFERENCES

ARIS, R. 1956 On the dispersion of a solute in a fluid flowing through a tube. *Proc. R. Soc.* A **235**, 67–77.

BOHN, D. J., MIYASAKA, K., MARCHAK, B. E., THOMPSON, W. K., FROESE, A. B. & BRYAN, A. C. 1980 Ventilation by high-frequency oscillation. *J. Appl. Physiol.* **48**, 710–716.

BUTLER, J. P. 1977 The Green's function for the convection-diffusion equation in an analytic lung model. *Bull. Math. Biol.* **39**, 543–563.

CHATWIN, P. C. 1975 On the longitudinal dispersion of passive contaminant in oscillatory flows in tubes. *J. Fluid Mech.* **71**, 513–527.

DANCKWERTS, P. V. 1953 Continuous flow systems: distributions of residence times. *Chem. Engng Sci.* **2**, 1–13.

DECKWER, W.-D. & MÄHLMANN, E. A. 1976 Boundary conditions of liquid phase reactors with axial dispersion. *Chem. Engng J.* **11**, 19–25.

DRAGON, C. A. & GROTBERG, J. B. 1991 Oscillatory flow and mass transport in a flexible tube. *J. Fluid Mech.* **231**, 135–155.

DRAZEN, J. M., KAMM, R. D. & SLUTSKY, A. S. 1984 High-frequency ventilation. *Physiol. Rev.* **64**, 505–543.

ECKMANN, D. M. & GROTBERG, J. B. 1988 Oscillatory flow and mass transport in a curved tube. *J. Fluid Mech.* **188**, 509–527.

ERDOGAN, M. E. & CHATWIN, P. C. 1967 The effects of curvature and buoyancy on the longitudinal dispersion of solute in a horizontal tube. *J. Fluid Mech.* **29**, 465–484.

GODLESKI, D. A. & GROTBERG, J. B. 1988 Convection-diffusion interaction for oscillatory flow in a tapered tube. *J. Biomech. Engng* **110**, 283–291.

HARRIS, H. G. & GOREN, S. L. 1967 Axial diffusion in a cylinder with pulsed flow. *Chem. Engng Sci.* **22**, 1571–1576.

HASELTON, F. R. & SCHERER, P. W. 1982 Flow visualization of steady streaming in oscillatory flow through a bifurcating tube. *J. Fluid Mech.* **123**, 315–333.

HUGHES, J. M. B., HOPPIN, F. G. & MEAD, J. 1972 Effect of lung inflation on bronchial length and diameter in excised lungs. *J. Appl. Physiol.* **32**, 25–35.

HYDON, P. E. 1991 Modelling the pulmonary circulation and gas transport in the lung. Ph.D. thesis, Cambridge University.

JAN, D. L., SHAPIRO, A. H. & KAMM, R. D. 1989 Some features of oscillatory flow in a model bifurcation. *J. Appl. Physiol.* **67**, 147–159.

JOHNSON, M. & KAMM, R. D. 1986 Numerical studies of steady flow dispersion at low Dean number in a gently curving tube. *J. Fluid Mech.* **172**, 329–345.

JOSHI, C. H., KAMM, R. D., DRAZEN, J. M. & SLUTSKY, A. S. 1983 Gas exchange in laminar oscillatory flows. *J. Fluid Mech.* **133**, 245–254.

KAMM, R. D., BULLISTER, E. T. & KERAMIDAS, C. 1986 The effect of a turbulent jet on gas transport during oscillatory flow. *J. Biomed. Engng* **108**, 266–272.

LYNE, W. H. 1971 Unsteady viscous flow in a curved pipe. *J. Fluid Mech.* **45**, 13–31.

NUNGE, R. J., LIN, T.-S. & GILL, W. N. 1972 Laminar dispersion in curved tubes and channels. *J. Fluid Mech.* **51**, 363–383.

PEDLEY, T. J. & KAMM, R. D. 1988 The effect of secondary motion on axial transport in oscillatory tube flow. *J. Fluid Mech.* **193**, 347–367.

SCHROTER, R. C. & SUDLOW, M. F. 1969 Flow patterns in models of the human bronchial airways. *Resp. Physiol.* **7**, 341–355.

SECOMB, T. W. 1978 Flow in a channel with pulsating walls. *J. Fluid Mech.* **273**, 273–288.

SHARP, M. K., KAMM, R. D., SHAPIRO, A. H., KIMMEL, E. & KARNIADAKIS, G. E. 1991 Dispersion in a curved tube during oscillatory flow. *J. Fluid Mech.* **223**, 537–563.

SLUTSKY, A. S., DRAZEN, J. M., INGRAM, R. H., KAMM, R. D., SHAPIRO, A. H., FREDBERG, J. J., LORING, S. H. & LEHR, J. 1980 Effective pulmonary ventilation with small volume oscillations at high frequency. *Science* **209**, 609–611.

SLUTSKY, A. S., KAMM, R. D. & DRAZEN, J. M. 1985 Alveolar ventilation at high frequencies using tidal volumes smaller than the anatomical dead space. In *Gas Mixing and Distribution in the Lung* (ed. L. A. Engel & M. Paiva). Marcel Dekker.

SMITH, R. 1988 Entry and exit conditions for flow reactors. *IMA J. Appl. Maths* **41**, 1–20.

TAYLOR, G. I. 1953 Dispersion of soluble matter in solvent flowing slowly through a tube. *Proc. R. Soc. Lond.* A **219**, 186–203.

WATSON, E. J. 1983 Diffusion in oscillatory pipe flow. *J. Fluid Mech.* **133**, 233–244.

WEHNER, J. F. & WILHELM, R. H. 1956 Boundary conditions of flow reactor. *Chem. Engng Sci.* **6**, 89–93.

WEIBEL, E. 1963 *Morphometry of the Human Lung*. Academic.

WEIS-FOGH, T. 1964 Diffusion in insect wing muscle, the most active tissue known. *J. Exp. Biol.* **41**, 229–256.